

Laser LIGA for Nickel Microheaters

by

Hengyi Jin

A/Prof Erol Harvey

Professor Derry Doyle, School of Engineering and Science, SUT

Abstract

This research and development has been carried out at IRIS in collaboration with the CRC for Micro Technology. The work commenced in May 2001 and completed in March 2002. This paper presents a sequential process development to fabricate Nickel microheaters based on Excimer laser micromachining, and microheater testing results. The objective is to explore the laser LIGA process to create Nickel microstructures as durable heating elements. By choosing printed circuit materials, such as PCB and Laminar AX dry film, the work resulted in an advanced process, which also included the localised photoresist removal by excimer laser and Cu selective etching. Using this process, we have achieved Nickel microheaters with suspended heating elements (serpentine shape), of which the smaller cross-section is less than $10\ \mu\text{m} \times 10\ \mu\text{m}$. All the microheaters have been tested in air with the DC current as the input variable. The systematic results for five typical Nickel microheaters have also been summarised in this paper. These results have indicated many technical and commercialisation potentials in microsystem technology field.

1. Introduction

Integration of heater elements in micro electro mechanical systems (MEMS) enables a whole range of sensors and actuators applications (Witvrouw, 1999). Some examples include absolute-humidity measurement (Kimura, 1995), gas sensor (Lee et al, 1995) and biomedical applications (Wise, 1997). These devices are mainly based on silicon, polysilicon or ceramics to create their structures, which incorporate some heating function (Rosa *et al.*, 1997). Candidate metals for microheaters have been identified (Yorshige, 1996), however most devices have been made using either surface micromachining (thin film) or its combination with silicon bulk micromachining. It is generally difficult to use these processes to realise durable thick metal features. Recently there has been growing interest in LIGA processes where the X-ray lithography step is replaced by a cheaper, lower resolution alternative such as UV photolithography ("poor man's LIGA") or laser photoablation (Holmes, 1997). In addition to the processes, there has also been search for cheaper materials. Printed Circuit Boards (PCB) have been, of late, adopted as the cheaper alternative to silicon wafers as substrates for MEMS application. This will allow hybrid integration of both electronic and fluidic components at low costs. Hence there has been increasing interest in using PCB as substrate for many micro device applications.

2. Industrial Implications

- Potentially practical for the microfabrication of MEMS devices based on printed circuit boards (PCBs)
- Functional examples include: microheaters, temperature sensors, flow rate sensors, electrothermally pneumatic micropumps, microcantilevers, microresonators and microrelays.

3. Experimental

3.1 Sample preparation

The detailed sample preparation and excimer laser system have been described in previous work (Jin, 2001a and Jin, 2001b). In this work, all the samples were prepared just based on Printed Circuit Board (PCB) with 30 μm copper clad. Each sample was then coated using 35 μm thick Laminar AX dry film photopolymer (Dynachem Inc., USA). Lamination was carried out using a Dynachem laminator. Micromachining was performed using an excimer laser projection system (Exitech Series 8000) equipped with a Lambda Physik LPX210i laser source, which was operated at 248 nm (KrF) in pulsed mode.

3.2 Laser patterning

A chrome-on-quartz mask was prepared in advance. The mask includes two circular patterns to be used for the electrical contact pads, and three serpentine shape patterns to be selected to create a heating element. Each of the three serpentine sets includes the left lead-in part, the right lead-out part, and a central repeating block of serpentes. This arrangement allows the designer to readily change the total length of the serpentine track between the pads simply by rewriting the laser CNC program to repeat the central block of serpentes without the need to use a new mask. This means that the maximum width of the serpentine structure is limited to the maximum translation distance of the workpiece stages, 200 mm in our case. When imaged onto the workpiece using the 1:10 lens, the mask produced contact pads 900 μm in diameter, and serpentine tracks that were 50 μm , 20 μm or 10 μm wide depending upon the mask set used. To prepare the polymer moulds for microstructures, the laser fluence and the number-of-laser-pulses needed to be determined. The criteria to identify the proper laser parameters were: (1) the laser ablation just penetrated the laminated dry film without noticeable seed layer damage as viewed using an optical microscope; (2) the ablated wall angle was sufficient to resolve the finest features. Criteria (1) drives one to use the lowest possible fluence, while criteria (2) forces one to use the highest possible fluence (Harvey, 1995). After the optimal laser conditions were determined, laser patterning was carried out to produce the polymer mould for the whole micro structure pattern.

3.3 Ni micro electroforming

The above polymer moulds were used to electroform Nickel microstructures with a standard Nickel sulfamate bath at a current density of $\sim 10 \text{ mA/cm}^2$. The bath was maintained at 47°C and $\sim \text{pH } 3$, and agitated by stirring within the beaker. The total Ni thickness was controlled by timing the electrodeposition, having established that the average Ni growth rate was about $10 \mu\text{m/hr}$ here.

3.4 Dry film removal, Cu selective etching and microscopy

Acetone, 10% NaOH and excimer laser ablation were each used separately, or sequentially, to remove the dry film photoresist after Ni micro electroforming. The dry film photoresist had been exposed to a varying extent since no special lighting precautions were used when handling and ablating the layer. Thus the usual NaOH chemical removal technique was a less reliable stripping process than it would normally have been. Hence, in this instance, we have used laser to remove the polymer in between the Nickel structures within the heating element. The Cu seed layer should also be removed since it short-circuits the electroformed structure if allowed to remain. To selectively remove Cu in the presence of fine Ni features, Cu etching was carried out after dry film removal. An etchant prepared with ($\sim 20 \text{ wt}\%$) ammonium persulfate was used for this purpose. Using this etchant, the Cu layer over most of the exposed area was removed, and the Ni serpentine features were released. However, there was a slight undercut beneath the contact pads. The resulting micro electroformed structures were observed using an optical microscope (Olympus BX 60), a Scanning Electron microscope (JEOL JSM – 35), and for 3D measurement and surface analysis, a confocal laser scanning microscope (Olympus OLS 1100).

4. Results And Discussions

4.1 Fabrication process

The optimal laser parameters and the characteristics of resultant polymer moulds have been presented in Table. 1. The excimer laser conditions indicated in the table represent the fluence and number of shots to machine the mould and also clean the surface of the seed layer.

Mask pattern size (μm)	Laser parameters		Polymer moulds	
	Fluence (J/cm^2)	Number of pulses	Aspect ratio	Side-wall angle
900 (contact pads)	1.5	40 + 5	<0.039	< 9°
50 (Track width)	1.5	40 + 10	0.7	$9\text{-}10^\circ$
20 (Track width)	1.2	90 + 10	1.75	12°
10 (Track width)	1.2	140 + 10	3.5	13°

Table 1 – Optimal Excimer Laser Ablation

From table 1, it may be noted that the larger contact pads needed smaller number of pulses compared to the tracks. As the track width is decreased from 50 μm to 10 μm , the fluence has been reduced from 1.5 J/cm^2 to 1.2 J/cm^2 , while the number of pulses increased dramatically. This was essential in this case, to achieve higher aspect ratio, while maintaining the wall angle at a reasonable value. At higher fluences, it was observed that the laminar layer in the gaps (between the track moulds) tends to be machined, which resulted in reduced aspect ratios. However, as the number of shots increased at a lower fluence, the wall angle increases. Hence, the values indicated in the table are chosen as a trade-off, which resulted in track moulds with acceptable aspect ratios and side wall angles as shown in the table. Electrodeposition was performed on the completed ablated structures. Typical patterned and electroformed structures with 50, 20 and 10 μm (nominal widths) wide tracks were shown in Fig.1 (a, b & c) respectively. The contact pads have the same dimensions in all the three cases.

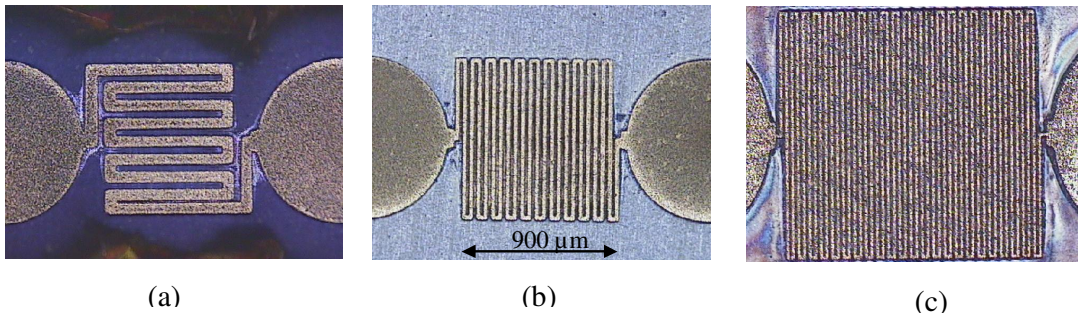


Figure 1- Top view of the 20 μm thick Electroformed Nickel patterns with (a) 50, (b) 20

After the electroforming, the photoresist between the tracks was removed, in order to facilitate the etching of copper layer beneath. It has been found that the clean removal of the resist in these gaps between the fine electroformed Ni tracks seems to be difficult especially following the chemical route using acetone or conventional hydroxide based strippers/etchants. This is clearly demonstrated in our study using three different thicknesses (8 μm , 16 μm , and 25 μm) of Ni tracks (20 μm wide). It was observed that the thicker the electroformed Ni feature, the more dry film remained between the features. Possible reasons for this include photoresist exposure by side scattered laser light or by room light during handling.

To solve this problem, the excimer laser has again been used for the removal of these dry film segments between tracks. The mask was removed from the laser beam line, and the workpiece held stationary during ablation. This removal also required the optimisation of the laser parameters. The laser conditions presented in table.2 were used for this purpose.

As discussed earlier, three different track widths (or gap between the tracks) viz., 50, 20 and 10 μm were considered in this analysis. However, it may be noted that 20 μm features were plated to three different thicknesses 21, 7 and 5 μm to achieve

different resistance values. The parameters a, b and h given in table.2 were represented as shown in Fig.2. From the table, it is clear that as the plated structure thickness decreased, the number of shots required to remove the resist between the tracks also reduced. For example, in case of 20 μm wide features, as the thickness reduced from 21 μm to 7 μm , both the fluence as well as the number of shots were reduced to completely remove the polymer but not damage the nickel feature or seed layer.

Table 2: Laser parameters used to remove polymer between serpentine Nickel tracks

Gap between the Ni tracks (μm)	Cross-section sizes of Nickel features (μm)			Excimer laser parameters	
	a	b	h	Fluence (J/cm^2)	Laser pulses
50	50	45	21	1.5	60 + 10
20	20	11	21	1.5	70 + 10
20	14	11	7	1.2	60 + 5
20	13	11	5	1.2	50 + 5
10	7	3	9	1.2	60 + 5

Table 2 – Laser Parameters Used to Remove Polymer Between Serpentine Nickel Tracks

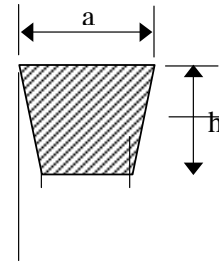


Figure 2 – Schematic of the Cross-Section View of Ni Tracks

During these “Maskless” laser trials, we observed a modification of the surface of the electroformed Ni pattern, as shown in Figure 4 (compared with Figure 3). Using a scanning laser confocal microscope, we measured the Ni surface roughness R_a to be 1.20 μm for the original electroformed Ni surface, but 0.193 μm for the same surface after the above excimer laser exposure.

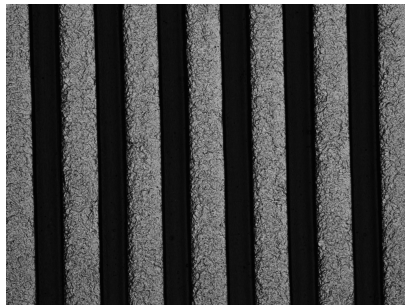


Figure 3 - Original electroformed Ni surface

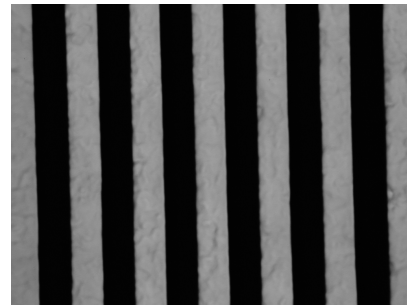


Figure 4 - After irradiation by excimer laser

This was followed by the selective etching of copper layer without affecting the top Nickel electroformed serpentine structure. Using a 20 wt% ammonium per sulphate solution, it takes approximately two hours to etch the 30 μm thick copper layer. Irrespective of the width or thickness of the tracks on the top, sacrificial copper etching has taken similar time periods. This is understandable due to the isotropic nature of the etching process with this etchant. During this process, nickel structures were totally unaffected and consequently their thickness remained unchanged.

4.2 Testing results

Typical Nickel serpentine structures with 50 μm and 20 μm wide structures, after the seed layer release are shown in Figure 5. These structures were bonded to 80 μm diameter copper wire using soldering as well as wire bonding techniques.

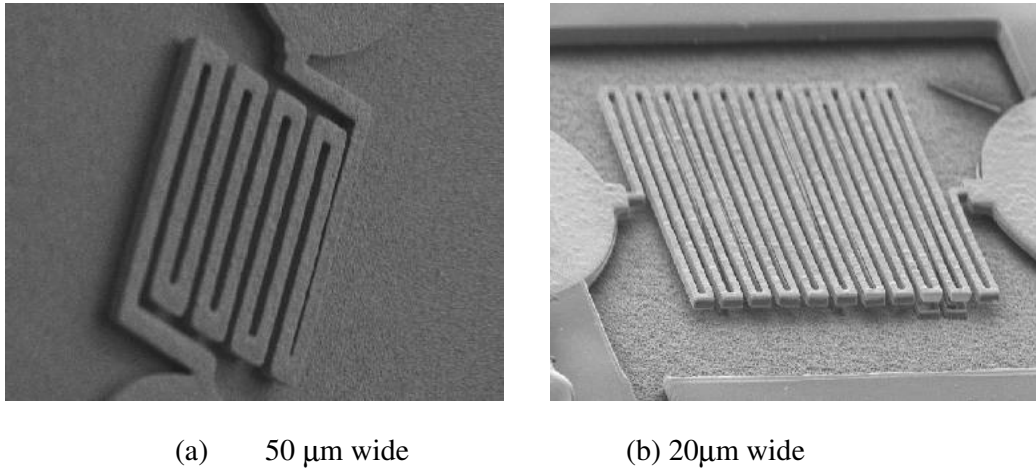


Figure 5 - released Nickel microheater structures after etching the copper layer underneath

The current vs voltage characteristics of these microheater structures were studied as a function of resistance, track size and temperature, using a constant current power supply. In figure 6, it can clearly be seen that as the heater resistance increased, the voltage has raised quicker, limiting the maximum current that can be applied to the heating element. It may be noted that the maximum current values indicated for each heater represent the maximum current than can be applied to the element without causing any damage. However, maximum current applied to the heating element with room temperature resistance of 15.85 ohms is an exception for this, which has not been tested till the limiting current value. The variation of the power as a function of current is shown in Fig.7. It may be noted from the figure that the maximum power (~260mw) could be applied to the heating element with a R_o of 4.45 ohms. The dimensions of this heating element a, b and h are 20, 11 and 21 μm respectively. It is also interesting to note that the two elements with extreme resistance values (0.5 ohms and 58.2 ohms) showed similar limiting power values.

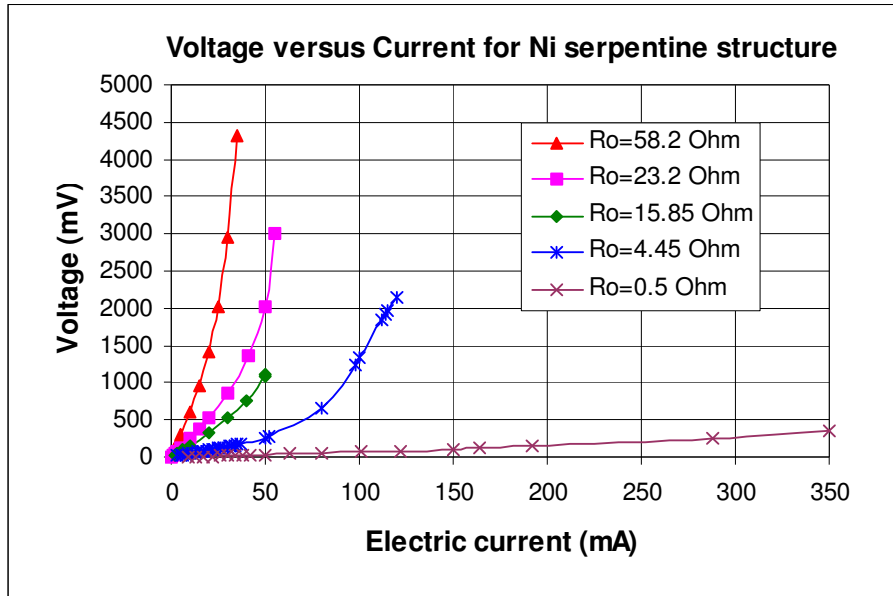


Figure 6 - Current -Voltage characteristics of microheaters with different initial resistance

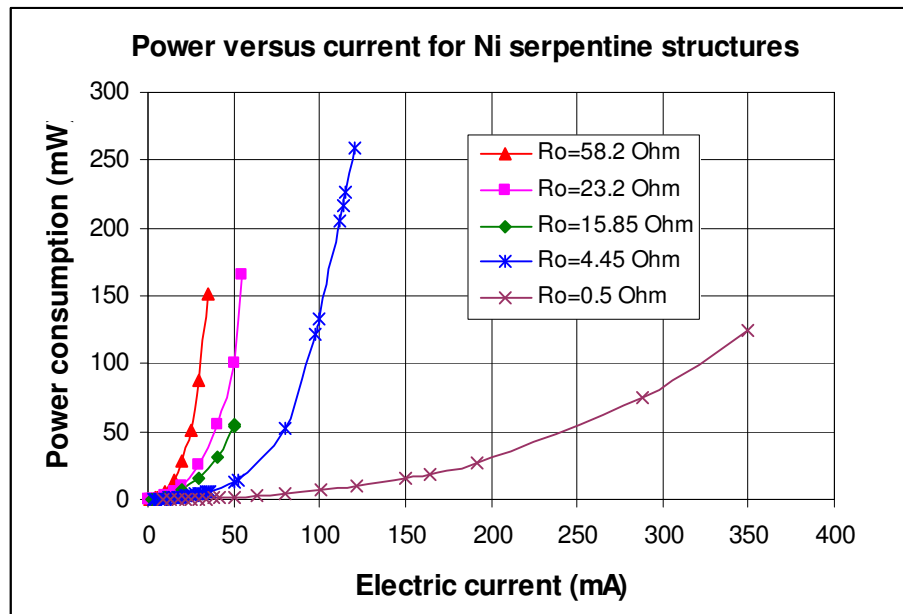


Figure 7 - Variation of power with resistance of the heaters for tracks of different widths

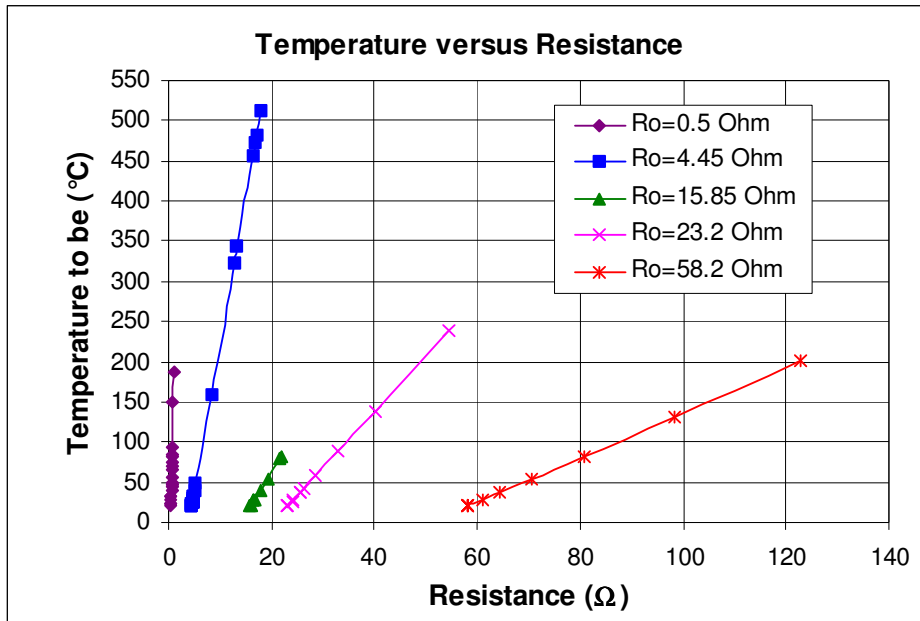


Figure 8: Variation of temperature with resistance of the heating element

In Figure 8, the relationship between the resistance and temperature of different elements fabricated in this study is shown. The temperature value is obtained using the simple relationships given below.

$$R_t = R_o \times [1 + \alpha \times (T - T_o)]$$

Assuming a room temperature, $T_o = 20\text{ }^\circ\text{C}$ and for Nickel, $\alpha = 6.15 \times 10^{-3}\ \Omega/\Omega\text{ }^\circ\text{C}^{-1}$,

$$T = T_o + \frac{1}{\alpha \times R_o} \times (R_t - R_o), \text{ where } R_t \text{ is the resistance at any temperature } T.$$

It is clear from this figure, that the temperature is limited by the maximum current and voltage values, which in turn depend on the individual resistance of the heating element. In this particular case, the heater with ($R_o = 0.5\text{ ohms}$, $a=50\mu\text{m}$) can be used up to a maximum temperature of 200°C . As was observed in the earlier graph, the elements with dimensions on two extremes of the values used in this study, showed similar maximum temperatures. This can be explained based on the current densities at respective powers applied to the elements. In this respect, the heating element with a R_t of 4.45 ohms achieved the maximum temperature.

5. Conclusion

This work clearly demonstrated the feasibility of fabricating the microheaters of different dimensions using Laser-LIGA technology using a PCB substrate especially suitable for microfluidic applications. Nickel heating elements of different dimensions were fabricated. These elements with serpentine structure were released by etching the sacrificial copper layer on the PCB. These suspended structures were tested for their current-voltage and resistance-temperature characteristics. It was found that around 20 μ m wide and 20 μ m thick structures appear to be the best choice for achieving the maximum temperature, within the optimal current and voltage values. This work also showed that excimer laser can be used for not only the initial patterning of the resist but also for the final removal of the resist after plating. The surface smoothening effect accompanying this laser based removal process has been perceived to be the additional advantage with this technique. Since the processes described are compatible with traditional surface or bulk micromachining, they can be used in combination with these techniques to realise thick electroformed LIGA-like structures.

6. Acknowledgments

The authors would like to express their to the CRC for Micro Technology of Australia for the financial support. Thanks also to Mr Martin Lloyd-Diviny, who helped with the Olympus confocal laser scanning microscope and Mr. Brian Dempster for his technical assistance.

7. References

A Witvrouw, V Simons, I Wolf, De P Moor, "The Fabrication and Reliability Testing of Ti/TiN Heaters", Proc. Of SPIE, Vol. 3874, 1999.

Mitsuteru Kimura, "New method to measure the absolute-humidity independently of the ambient temperature", Piscataway, NJ, USA. IEEE, 1995.

Duk-Dong Lee et al. "Low power micro gas sensor, Piscataway", NJ, USA. IEEE, 1995.
Kensall D Wise, Jingkuang Chen, "Silicon probe with integrated micrometers for thermal marking and monitoring of neural tissue", IEEE Transactions on Biomedical Engineering, Vol. 44, pp770-774, 1997.

M A Rosa et al. "Fabrication and analysis of silicon microbridge heaters micromachined from (100) SOI wafers, Piscataway", NJ, USA. IEEE, 1997.

Ishii Yorshige Matoba Hirotsugu and Inui Tetsuya Hirata Susumu, "An ink - jet Head Using Diaphragm Microactuator", IEEE, 1996.

A S Holmes, S M Saidam and R A Lawes, "Low cost LIGA processes", Stevenage, Engl. IEE, 1997.

Hengyi Jin, Muralidhar K Gantasala, Jason P Hayes, Karlo Jolic and Erol C Harvey, "Laser micromachining and Nickel-plating of high aspect ratio structures in polymer moulds", Proc. Of SPIE, Vol. 4236, pp222-228, 2001.

Hengyi Jin, Erol Harvey et al, "Laser-LIGA for Serpentine Ni Microstructures", Proc. Of SPIE, Vol. 4592, pp166-171, 2001.

Erol C Harvey, Phil T Rumsby, Malcolm C Gower and Jason L Remnant, "Microstructuring by Excimer Laser", Proc. Of SPIE, Vol. 2639, pp266-276, 1995.